Inorg. Chem. **2002**, *41*, 958–966

Heterometal Cubane-Type MFe_3S_4 Clusters (M = Mo, V) Trigonally Symmetrized with Hydrotris(pyrazolyl)borate(1–) and Tris(pyrazolyl)methanesulfonate(1–) Capping Ligands

Dmitry V. Fomitchev, Craig C. McLauchlan, and R. H. Holm*

Department of Chemistry and Chemical Biology, Harvard University, Cambridge, Massachusetts 02138

Received October 24, 2001

A series of heterometal cubane-type clusters containing $[VFe_3S_4]^{2+}$ and $[MoFe_3S_4]^{3+,2+}$ cores has been prepared. Ligand substitution of $[(DMF)_3VFe_3S_4Cl_3]^-$ affords $[(Tpms)VFe_3S_4L_3]^{2-}$ (L = Cl^- (**8**), EtS^- (**9**), *p*-$MeC_6H_4S^-$, *p*-$MeC_6H_4O^-$). A new procedure for the preparation of molybdenum single cubanes is introduced by the reaction of recently reported $[(Tp)MoS(S_4)]^-$ with $FeCl_2$/NaSEt to afford $[(Tp)MoFe_3S_4Cl_3]^-$ (**1**, 75% yield). This procedure is more efficient that the existing multistep synthesis of single cubanes, which generally affords clusters of mirror symmetry. Also prepared were $[(Tp)MoFe_3S_4L_3]^-$ (L = EtS^- (**2**), *p*-$MeC_6H_4S^-$). Reduction of **1** with borohydride gives $[(Tp)MoFe_3S_4Cl_3]^{2-}$ (**5**, 67%). Owing to the nature of the heterometal ligand, all clusters have idealized trigonal symmetry, reflected in their ^1H NMR spectra. Trigonal structures are demonstrated by crystallography of (Bu_4N)[**1**,**2**], $(Bu_4N)_2$[**5**]·MeCN, and $(Me_4N)_2$[**8**,**9**]. The availability of **1** and **5** allows the first comparison of structures and ^{57}Fe isomer shifts of $[MoFe_3S_4]^{3+,2+}$ in a constant ligand environment. Small increases in most bond distances indicate that an antibonding electron is added in the reduction of **1**. Collective synthetic and electrochemical results from this and other studies demonstrate the existence of the series of oxidation states $[VFe_3S_4]^{3+,2+,1+}$ and $[MoFe_3S_4]^{4+,3+,2+}$ whose relative stabilities within a given series are strongly ligand dependent. Isomer shifts indicate that the reduction of **1** largely affects the Fe_3 subcluster and are consistent with the formal descriptions $[MoFe^{3+}{}_2Fe^{2+}S_4]^{3+}$ (**1**) and $[MoFe^{3+}Fe^{2+}{}_2S_4]^{2+}$ (**5**). Reaction of **1** with excess Li_2S in acetonitrile affords the double cubane $\{[(Tp)MoFe_3S_4Cl_2]_2(\mu_2\text{–}S)\}^{2-}$, whose sulfide-bridged structure is supported by two sequential reductions separated by 290 mV, in analogy with previously reported double cubanes of higher charge. Trigonally symmetric single cubanes eliminate isomers in the formation of double cubanes and other cluster structures, and may be of considerable value in the preparation of new types of M–Fe–S clusters. (Tpms = tris(pyrazolyl)methanesulfonate(1–); Tp = hydrotris(pyrazolyl)borate(1–).)

1. Introduction

Research in this laboratory on heterometal clusters containing the cubane-type $MFe_3(\mu_3\text{–}S)_4$ core has been largely motivated by the geometrical resemblance of their six-coordinate M = Mo and V sites[1,2] to those in the native clusters of nitrogenase,[3–6] and by the possibility of using these species as precursors in the synthesis of clusters related to those in the enzyme. In one approach, the edge-bridged double cubanes $[(Cl_4cat)_2(R_3P)_2Mo_2Fe_6S_8(PR_3)_4]$[7] (R = Et,[8,9] Pr;[10] see Chart 1 for abbreviations) react with carbon monoxide under pressure to afford cuboidal $MoFe_3S_3$ clusters whose shape resembles the corresponding $MoFe_3S_3$ fragment

* To whom correspondence should be addressed. E-mail: holm@chemistry.harvard.edu.

(1) Holm, R. H. *Adv. Inorg. Chem.* **1992**, *38*, 1−71.
(2) Malinak, S. M.; Coucouvanis, D. *Prog. Inorg. Chem.* **2001**, *49*, 599−662.
(3) Howard, J. B.; Rees, D. C. *Chem. Rev.* **1996**, *96*, 2965−2982.
(4) Peters, J. W.; Stowell, M. H. B.; Soltis, S. M.; Finnegan, M. G.; Johnson, M. K.; Rees, D. C. *Biochemistry* **1997**, *36*, 1181−1187.
(5) Smith, B. E. *Adv. Inorg. Chem.* **1999**, *47*, 160−218.
(6) Mayer, S. M.; Lawson, D. M.; Gormal, C. A.; Roe, S. M.; Smith, B. E. *J. Mol. Biol.* **1999**, *292*, 871−891.
(7) Allen, F. H.; Kennard, O. *Chem. Des. Autom. News* **1993**, *8*, 1, 31−37.
(8) Demadis, K. D.; Campana, C. F.; Coucouvanis, D. *J. Am. Chem. Soc.* **1995**, *117*, 7832−7833.
(9) Osterloh, F.; Segal, B. M.; Achim, C.; Holm, R. H. *Inorg. Chem.* **2000**, *39*, 980−989.
(10) Han, J.; Beck, K.; Ockwig, N.; Coucouvanis, D. *J. Am. Chem. Soc.* **1999**, *121*, 10448−10449.

10.1021/ic011106d CCC: $22.00
Published on Web 02/01/2002

Chart 1. Abbreviations and Designations of MFe_3S_4 Complexes

$[(Tp)MoFe_3S_4Cl_3]^-$	**1**
$[(Tp)MoFe_3S_4(SEt)_3]^-$	**2**
$[(Tp)MoFe_3S_4(S\text{-}p\text{-}tol)_3]^-$	**3**
$\{[(Tp)MoFe_3S_4Cl_2]_2(\mu_2\text{-}S)\}^{2-}$	**4**
$[(Tp)MoFe_3S_4Cl_3]^{2-}$	**5**
$[(DMF)_3VFe_3S_4Cl_3]^-$	**6**[22,23]
$[(Tp)VFe_3S_4Cl_3]^{2-}$	**7**[14,24]
$[(Tpms)VFe_3S_4Cl_3]^{2-}$	**8**
$[(Tpms)VFe_3S_4(SEt)_3]^{2-}$	**9**
$[(Tpms)VFe_3S_4(S\text{-}p\text{-}tol)_3]^{2-}$	**10**
$[(Tpms)VFe_3S_4(O\text{-}p\text{-}tol)_3]^{2-}$	**11**
$[(Meida)MoFe_3S_4Cl_3]^{2-}$	**12**[15,19]
$[(Tp)MoS(S_4)]^-$	**13**[27]
$\{[(Meida)MoFe_3S_4Cl_2]_2(\mu_2\text{-}S)\}^{4-}$	**14**[15]

Abbreviations: cat = catecholate(2-), Cl_4cat = tetrachlorocatcholate(2-), LS_3 = 1,3,5-tris((4,6-dimethyl-3-mercapto-phenyl)thio)-2,4,6-tris(*p*-tolylthio)benzene(3-), Meida = methylimidodiacetate(2-), pz = pyrazolyl, solv = solvate molecule, tol = tolyl, Tp = hydrotris(pyrazolyl) borate(1-), Tp*, hydrotris(3,5-dimethylpyrazolyl)borate(1-), Tpms = tris(pyrazolyl-methane)sulfonate(1-)

of the $MoFe_7S_9$ core of the iron−molybdenum cofactor.[10,11] The same cluster (R = Et) upon reaction with hydrosulfide under reducing conditions has been shown to form larger clusters containing the $Mo_2Fe_6S_9$ fragment with a topology closely resembling the P^N cluster of nitrogenase.[12,13] The recently prepared double cubane $[(Tp)_2V_2Fe_6S_8(PEt_3)_4]$,[14] also edge-bridged, may have a similar reactivity potential. By these means, topological analogues of part or all of the native clusters have been achieved, although not necessarily in physiological oxidation states.

In a second approach to the cofactor cluster, bridged double cubane clusters with the core unit $\{[MoFe_3S_4]_2(\mu_2\text{-}S)\}^{4+}$ are prepared, with the possibility (not yet realized) of induced skeletal rearrangement reactions to afford clusters with the core $Mo_2Fe_6S_9$.[15,16] Certain difficulties intervene in this approach. Single cubanes such as $[(L_3)MoFe_3S_4Cl_3]^z$, in which the molybdenum site is necessarily protected from reaction by chelation with generalized tridentate ligand L_3 in order to direct bridge formation to an iron site, are coupled with Li_2S to form the sulfide-bridged double cubanes $\{[(L_3)MoFe_3S_4Cl_2]_2S\}^{2z}$. At the time this work was initiated, appropriate starting single cubanes were available only by a multistep procedure from thiolate-bridged double cubanes,[15,17,18] themselves formed in self-assembly reactions. An attractive single cubane that was successfully coupled to form double cubanes is $[(Meida)MoFe_3S_4Cl_3]^{2-}$,[15,19] in which the methylimidodiacetate ligand of type L_2L' affords a cluster of C_s symmetry. Coupling of two such clusters leads to the double cubane $\{[(Meida)MoFe_3S_4Cl_2]_2S\}^{4-}$, which can exist as a mixture of four geometrical isomers. ^{1}H NMR spectra clearly indicate the formation of isomers in this and other double cubanes carrying the Meida ligand.[15,16] Further, successful conversion of an isomeric double cubane to a cluster with cofactor topology such as $[(Meida)_2Mo_2Fe_6S_9]$ will potentially lead to a mixture of two geometrical isomers.

To avoid isomeric mixtures with the attendant difficulties in purification and crystallization of products, we have sought trigonally symmetric MFe_3S_4 single cubanes with heterometals M = Mo, V. Because of their greater complexity and deviation from cofactor composition, trigonal clusters with single metals attached exo to the heterometal[20,21] are unsuitable as starting materials. Trigonally symmetric VFe_3S_4 clusters with a protected vanadium site are readily accessible because of the ease of substitution of DMF ligands in the trigonal cluster $[(DMF)_3VFe_3S_4Cl_3]^-$.[22] This matter is illustrated by the formation of the hydrotris(pyrazolyl)borate cluster $[(Tp)VFe_3S_4(LS_3)]^{2-}$ from $[(DMF)_3VFe_3S_4(LS_3)]^-$ [23] and, subsequently, the preparation of $[(Tp)VFe_3S_4Cl_3]^{2-}$,[24] which has been recently shown to undergo ligand substitution and redox reactions to afford, among other products, the aforementioned $V_2Fe_6S_8$ double cubane. The situation with $MoFe_3S_4$ clusters is, however, more difficult. The only feasible means of introducing tridentate ligands at the Mo site has been ligand substitution of the catecholate ligand in, usually, $[(Cl_4cat)(solv)MoFe_3S_4Cl_3]^{2-}$ by reaction with the protonated ligand at elevated temperature, as in the formation of $[(Meida)MoFe_3S_4Cl_3]^{2-}$ with release of the ligand as the catechol.[19] We have not been able to devise a clean reaction system leading to a trigonally symmetric $MoFe_3S_4$ product by such means. In this work, we report the synthesis, structures, and selected properties of trigonally symmetric molybdenum and vanadium clusters, for use in subsequent cluster synthesis and other applications, in which the molybdenum and vanadium atoms are bound by hydrotris(pyrazolyl)borate(1−) and tris(pyrazolyl)methanesulfonate-(1−), respectively. As part of this investigation, we describe a more direct pathway than heretofore to $MoFe_3S_4$ single cubanes.

Experimental Section

Preparation of Compounds. All procedures were carried out under a pure dinitrogen atmosphere using standard Schlenk and glovebox techniques. Ether and acetonitrile were passed through an Innovative Technologies solvent purification system. Methanol was distilled over magnesium, and toluene was distilled from

(11) Tyson, M. A.; Coucouvanis, D. *Inorg. Chem.* **1997**, *36*, 3808−3809.
(12) Osterloh, F.; Sanakis, Y.; Staples, R. J.; Münck, E.; Holm, R. H. *Angew. Chem., Int. Ed.* **1999**, *38*, 2066−2070.
(13) Osterloh, F.; Achim, C.; Holm, R. H. *Inorg. Chem.* **2001**, *40*, 224−232.
(14) Hauser, C.; Bill, E.; Holm, R. H. *Inorg. Chem.*, in press.
(15) Huang, J.; Mukerjee, S.; Segal, B. M.; Akashi, H.; Zhou, J.; Holm, R. H. *J. Am. Chem. Soc.* **1997**, *119*, 8662−8674.
(16) Huang, J.; Holm, R. H. *Inorg. Chem.* **1998**, *37*, 2247−2254.
(17) Armstrong, W. H.; Mascharak, P. K.; Holm, R. H. *J. Am. Chem. Soc.* **1982**, *104*, 4373−4383.
(18) Mascharak, P. K.; Armstrong, W. H.; Mizobe, Y. *J. Am. Chem. Soc.* **1983**, *105*, 475−483.
(19) Demadis, K. D.; Coucouvanis, D. *Inorg. Chem.* **1995**, *34*, 436−448.
(20) Wolff, T. E.; Berg, J. M.; Holm, R. H. *Inorg. Chem.* **1981**, *20*, 174−180.
(21) Barrière, F.; Evans, D. J.; Hughes, D. L.; Ibrahim, S. K.; Talarmin, J.; Pickett, C. J. *J. Chem. Soc., Dalton Trans.* **1999**, 957−964.
(22) Kovacs, J. A.; Holm, R. H. *Inorg. Chem.* **1987**, *26*, 702−711.
(23) Ciurli, S.; Holm, R. H. *Inorg. Chem.* **1989**, *28*, 1685−1690.
(24) Malinak, S. M.; Demadis, K. D.; Coucouvanis, D. *J. Am. Chem. Soc.* **1995**, *117*, 3126−3133.

sodium/benzophenone ketyl. All solvents were further deoxygenated prior to use. The compounds $K[HB(C_3H_3N_2)_3]$ [25] (KTp) and $(Et_4N)[(Tp)Mo(CO)_3]$ [26] were prepared by published methods. $(Bu_4N)[(Tp)MoS(S_4)]$ was prepared by a procedure analogous to that for the Et_4N^+ salt.[27]

$(Et_4N)[(Tp)MoFe_3S_4Cl_3]$. To a pink solution of 453 mg (3.57 mmol) of $FeCl_2$ in 4 mL of methanol was added a solution of 302 mg (3.61 mmol) of NaSEt in 1 mL of methanol to afford a yellow-ochre solution. To this solution was added a dark green solution of 704 mg (1.18 mmol) of $(Et_4N)[(Tp)MoS(S_4)]$ [27] in 45 mL of acetonitrile. After 1 min, 319 mg (1.21 mmol) of PPh_3 was added to the reaction mixture. The reaction mixture was stirred for 16 h, filtered through a medium frit to remove a white solid, and the brown filtrate was reduced to dryness in vacuo. The residue was thoroughly washed with toluene and ether and dried in vacuo. The product was isolated as 740 mg (75%) of black needles after two recrystallizations from acetonitrile/ether. Absorption spectrum (acetonitrile; λ_{max} (ϵ_M)): 256 (24 600), 321 (9700) nm. IR (KBr): ν_{BH} 2515, 2493 cm^{-1}. EPR (DMF/MeCN): $g \approx 5.62, 2.07$. ^1H NMR (CD_3CN, anion): δ 17.11 (1), 14.0 (br, 1), 6.50 (1), 4.3 (br q, B−H). Anal. Calcd for $C_{17}H_{30}BCl_3Fe_3MoN_7S_4$: C, 24.27; H, 3.59; Cl, 12.64; Fe, 19.91; Mo, 11.40; N, 11.65; S, 15.25. Found: C, 24.48; H, 3.64; Cl, 12.78; Fe, 19.94; Mo, 11.59; N, 11.75; S, 15.35. Black needles of $(Bu_4N)[(Tp)MoFe_3S_4Cl_3]$ were prepared in an analogous fashion with $(Bu_4N)[(Tp)MoS(S_4)]$ instead of the Et_4N^+ salt.

$(Bu_4N)_2[(Tp)MoFe_3S_4Cl_3]$. A solution of 156 mg (0.163 mmol) of $(Bu_4N)[(Tp)MoFe_3S_4Cl_3]$ in 3 mL of acetonitrile was added to an ampule containing 43.4 mg (0.169 mmol) of $(Bu_4N)[BH_4]$ in 1 mL of acetonitrile. The green-black solution was stirred for 14 h, after which it was filtered through Celite and reduced to dryness in vacuo. The product was obtained as 136 mg (67%) as black crystalline blocks after recrystallization from acetonitrile/ether. Absorption spectrum (acetonitrile; λ_{max} (ϵ_M)): 303 (10 400), 390 (7300) nm. IR (KBr): ν_{BH} 2515, 2482 cm^{-1}. ^1H NMR (CD_3CN, anion): δ 19.07 (1), 18.2 (br, 1), 4.92 (1); the B−H proton was not located. Anal. Calcd for $C_{43}H_{85}BCl_3Fe_3MoN_9S_4$: C, 41.75; H, 6.93; Cl, 8.60; Fe, 13.54; Mo, 7.76; N, 10.19; S, 10.37. Found: C, 41.55; H, 6.78; Cl, 8.83; Fe, 13.36; Mo, 7.54; N, 10.24; S, 10.44. Brown needles of $(Et_4N)_2[(Tp)MoFe_3S_4Cl_3]$ may be prepared in an analogous fashion using Et_4N^+ salts of the initial cluster and the reductant; the compound was isolated in 87% yield.

$(Et_4N)[(Tp)MoFe_3S_4(SEt)_3]$. To a stirred solution of 105 mg (0.124 mmol) of $(Et_4N)[(Tp)MoFe_3S_4Cl_3]$ in 3 mL of acetonitrile was added 33 mg (0.383 mmol) of NaSEt. The solution turned from brown to red-brown within 2 min. After 20 h, the red-brown solution was filtered through Celite to remove NaCl and the red-brown filtrate was diluted with 15 mL of ether. The product was isolated as 65 mg (57%) of brown platelike crystals. Absorption spectrum (acetonitrile; λ_{max} (ϵ_M)): 265 (25900), 399 (14530) nm. ^1H NMR (CD_3CN, anion): δ 65.5 (br, CH_2), 15.04 (CH), 6.19 (CH), 5.67 (CH_3); one pyrazolyl and the B−H proton were not located. This compound was further identified by an X-ray structure determination.

$(Bu_4N)_2\{[(Tp)MoFe_3S_4Cl_2]_2S\}$. A solution of 252.5 mg (0.265 mmol) of $(Bu_4N)[(Tp)MoFe_3S_4Cl_3]$ in 3 mL of acetonitrile was added to an ampule containing 12.0 mg (0.261 mmol) of Li_2S. The reaction mixture was stirred for 14 h, filtered through Celite to remove excess of Li_2S and LiCl, and reduced to dryness in vacuo. The black polycrystalline solid was washed with ether and dried under vacuum to afford 226 mg (91%) of product. IR(KBr): ν_{BH} 2515, 2488 cm^{-1} ^1H NMR (CD_3CN, anion): δ 21.04 (1), 14.01 (2), 6.47 (2), 6.27(1), 4.2 (br, B−H); two pz protons were not located. Anal. Calcd for $C_{50}H_{92}B_2Cl_4Fe_6Mo_2N_{14}S_9$: C, 32.14; H, 4.96; Cl, 7.59; Fe, 17.93; Mo, 10.27; N, 10.50; S, 15.45. Found: C, 32.20; H, 5.04; Cl, 7.59; Fe, 17.78; Mo, 10.32; N, 10.42; S, 15.52.

$(Me_4N)_2[(Tpms)VFe_3S_4Cl_3]$. To a brown solution of 500 mg (0.56 mmol) of $(Me_4N)[(DMF)_3VFe_3S_4Cl_3]\cdot 2DMF$ [23] in 50 mL of acetonitrile, 189 mg (0.63 mmol) of lithium tris(pyrazolyl)-methanesulfonate[28] and 61 mg (0.56 mmol) of Me_4NCl were added. The mixture was stirred for 8 h and filtered. The red-brown filtrate was layered with 100 mL of ether and maintained at 5 °C. After 2 days, black crystals and a reddish crystalline impurity were isolated. The pure product was obtained as 190 mg (38%) of black crystals after recrystallization from acetonitrile/ether. Absorption spectrum (acetonitrile; λ_{max} (ϵ_M)): 320 (7230) nm. EPR (DMF/MeCN): $g \approx 5.64, 2.02$. ^1H NMR (CD_3CN, anion): δ 21.12 (1), 17.0 (br, 1), 4.80 (1). Anal. Calcd for $C_{18}H_{33}Cl_3Fe_3N_8O_3S_5V$: C, 24.17; H, 3.72; Cl, 11.89; Fe, 18.73; N, 12.52; V, 5.69. Found: C, 24.88; H, 3.77; Cl, 12.18; Fe, 19.35; N, 12.85; V, 6.05.

$(Me_4N)_2[(Tpms)VFe_3S_4(SEt)_3]$. To a solution of 50 mg (0.056 mmol) of $(Me_4N)_2[(Tpms)VFe_3S_4Cl_3]$ in 4 mL of acetonitrile was added 14 mg (0.167 mmol) of NaSEt. The solution was stirred for 15 h and filtered. The red-brown filtrate was diluted 20 mL of ether, causing separation of a black precipitate which was isolated, washed with ether, and dried in vacuo. Recrystallization from acetonitrile/ether afforded the product as 26 mg (48%) of black crystals. Absorption spectrum (acetonitrile; λ_{max} (ϵ_M)): 272 (16 800), 395 (11 900) nm. EPR (DMF/MeCN): $g \approx 5.97, 3.96, 2.07$. ^1H NMR (CD_3CN, anion): δ 56.6 (br, CH_2), 20.11 (CH), 18.0 (br,CH), 5.25 (CH_3), 4.44 (CH). This compound was further identified by an X-ray structure determination.

In the sections that follow, clusters are numerically designated as **1**−**14** according to Chart 1.

Other Compounds. The following compounds were prepared, their structures determined by X-ray methods, and selected properties determined. Because of their close similarities to the above compounds in synthesis, structure solution and refinement, and properties, reported characterization information is limited to crystallographic data (213 K).[29] (Et_4N)[**3**]: monoclinic, $P2_1/n$, $a = 12.176(5)$ Å, $b = 13.464(6)$ Å, $c = 29.38(1)$ Å, $\beta = 94.08(1)°$, $V = 4803(3)$ Å^3, $Z = 4$, R1 = 0.037, wR2 = 0.083. $(Et_4N)[(Tp^*)MoFe_3S_4Cl_3]$: triclinic, $P\bar{1}$, $a = 10.110(4)$ Å, $b = 10.387(4)$ Å, $c = 19.019(7)$ Å, $\alpha = 77.92(1)°$, $\beta = 75.75(1)°$, $\gamma = 81.44(1)°$, $V = 1833(1)$ Å^3, $Z = 2$, $R_1 = 0.041$, $wR_2 = 0.102$. $(Me_4N)_2$[**10**]: triclinic, $P\bar{1}$, $a = 10.657(1)$ Å, $b = 16.339(1)$ Å, $c = 17.398(1)$ Å, $\alpha = 74.19(1)°$, $\beta = 72.27(1)°$, $\gamma = 88.07(1)°$, $V = 2772(1)$ Å^3, $Z = 2$, $R_1 = 0.066$, $wR_2 = 0.136$. $(Me_4N)_2$[**11**]: monoclinic, Cc, $a = 13.155(1)$ Å, $b = 15.659(1)$ Å, $c = 24.004(1)$ Å, $\beta = 99.40(1)°$, $V = 4878(1)$ Å^3, $Z = 4$, $R_1 = 0.058$, $wR_2 = 0.135$.

X-ray Structure Determinations. The structures of the five compounds listed in Table 1 were determined. Suitable crystals of (Bu_4N)[**1**], $(Bu_4N)_2$[**5**]·MeCN, and $(Me_4N)_2$[**8**,**9**] were obtained by ether diffusion in acetonitrile solutions; crystals of (Bu_4N)[**2**] were obtained by ether diffusion into a THF solution. Crystals were mounted in Infineum oil on a fiber on a goniometer head which was placed in the dinitrogen cold stream of a Bruker AXS P3

(25) Trofimenko, S. *Inorg. Synth.* **1970**, *12*, 99−109.
(26) Trofimenko, S. *J. Am. Chem. Soc.* **1969**, *91*, 588−595.
(27) Seino, H.; Arai, Y.; Iwata, N.; Nagao, S.; Mizobe, Y.; Hidai, M. *Inorg. Chem.* **2001**, *40*, 1677−1682.
(28) Kläui, W.; Berghahn, M.; Rheinwald, G.; Lang, H. *Angew. Chem., Int. Ed.* **2000**, *39*, 2464−2466.
(29) See paragraph at the end of this article for Supporting Information available.

Table 1. Crystallographic Data[a]

	(Bu_4N)[**1**]	(Bu_4N)[**2**]	$(Bu_4N)_2$[**5**]·MeCN	$(Me_4N)_2$[**8**]	$(Me_4N)_2$[**9**]
empirical formula	$C_{25}H_{46}BCl_3Fe_3MoN_7S_4$	$C_{31}H_{61}BFe_3Mo\ N_7S_7$	$C_{43}H_{85}BCl_3Fe_3\ MoN_9S_4$	$C_{18}H_{33}Cl_3Fe_3N_{\ 8}O_3S_5V$	$C_{24}H_{48}Fe_3N_8O_3\ S_8V$
fw, g/mol	953.58	1030.59	1237.09	894.66	971.67
cryst syst	triclinic	monoclinic	monoclinic	orthorhombic	orthorhombic
space group	$P\bar{1}$	$P\ 2_1/n$	$P\ 2_1/n$	$P\ 2_12_12_1$	$P\ 2_12_12$
a, Å	10.205(2)	11.276(2)	13.718(1)	9.169(2)	19.553(1)
b, Å	11.452(2)	23.221(3)	29.809(3)	15.161(3)	20.406(1)
c, Å	19.570(4)	36.140(5)	15.988(2)	24.777(5)	10.220(1)
α, deg	92.04(3)	90.0	90.0	90.0	90.0
β, deg	103.88(3)	95.01(3)	113.48(1)	90.0	90.0
γ, deg	115.80(3)	90.0	90.0	90.0	90.0
V, Å^3	1973(1)	9427(2)	5996(1)	3444(1)	4078(1)
Z	2	8	4	4	4
ρ (calc), g/cm^3	1.605	1.452	1.370	1.725	1.583
2 *θ* range, deg	4.0−55.72	2.86−50.00	2.74−56.58	3.14−54.74	2.88−56.58
μ, mm^{-1}	1.834	1.505	1.225	2.073	1.715
GOF (F^2)	1.035	1.131	0.955	0.927	0.925
R_1[b] (wR_2[c])	0.049 (0.113)	0.074 (0.158)	0.058 (0.129)	0.033 (0.063)	0.043 (0.077)

[a] Data collected at 213 K with graphite monochromatized Mo Kα ($\lambda = 0.710\ 73$ Å) radiation. [b] $R_1 = \sum||F_o| - |F_c||/\sum|F_o|$. [c] $wR_2 = \{\sum[w(F_o^2 - F_c^2)^2/\sum w(F_o^2)^2]\}^{1/2}$.

diffractometer equipped with a 1 K CCD area detector and graphite-monochromated Mo Kα radiation. Data were collected at 213 K using the following strategy: 606 frames of 0.3° in *ω* with $\phi = 0°$, 435 frames of 0.3° in *ω* with $\phi = 90°$, and 235 frames of 0.3° in *ω* with $\phi = 180°$. An additional 50 frames of 0.3° in *ω* with $\phi = 0°$ were collected to allow for decay correction. For $(Me_4N)_2$-[**8**], data were collected at 213 K in 1215 frames of 0.3° in *ϕ* followed by 60 frames of 0.3° in *ω* with $\phi = 0°$, 40 frames of 0.3° in *ω* with $\phi = 90°$, and 30 frames of 0.3° in *ω* with $\phi = 180°$. An additional 50 frames of 0.3° in *ϕ* were collected to allow for decay correction. Data were processed with the program SAINT for integration; Lorentz, polarization, and decay corrections; and merging. The data were further corrected for frame variations and absorption with the program SADABS, which relies on redundancy in the data. Space groups were determined on the basis of systematic absences using the program XPREP. Structure solutions were found by direct methods and refined against F^2 with the use of full-matrix least-squares techniques with statistical weighting and anisotropic displacement parameters for all non-hydrogen atoms. In the final stages of refinement, hydrogen atoms were added at idealized positions and refined as riding atoms with a uniform value of U_{iso}. All least-squares refinements were done with the SHELXL-97 structure refinement package. Each crystal structure possesses well-separated cations and cluster anions. These complexes contain the well-studied MFe_3S_4 cubane core. The asymmetric unit of **1**, **5**, **8**, and **9** contains one single cubane unit, whereas the asymmetric unit of **2** contains two single cubane units. For $(Me_4N)_2$[**8**], one cation was modeled in two orientations. All other structures solved and refined routinely. Crystallographic details are summarized in Table 1.[29]

Other Physical Measurements. All measurements were performed under anaerobic conditions. ^{1}H NMR spectra were collected using a Varian AM-400 spectrometer. Cyclic voltammograms (100 mV/s) were recorded with a Princeton Applied Research Model 263 potentiostat/galvanostat using a Pt working electrode and 0.1 M $(Bu_4N)(PF_6)$ supporting electrolyte. Potentials are referenced to a saturated calomel electrode (SCE). Absorption spectra were recorded with a Cary 50 Bio spectrophotometer. IR spectra were determined with a Nicolet Nexus 470 FT-IR spectrometer. EPR spectra were obtained at 4.2 K in glasses (DMF/acetonitrile, 1:1 (v/v)) on a Bruker ESP 300E X-band spectrometer, equipped with a variable temperature accessory (manufactured by Oxford Instruments) and Hewlett-Packard 5350B microwave frequency counter. Mössbauer spectra were collected at 77 K with a constant-acceleration spectrometer. Data were analyzed using WMOSS software (WEB Research Co., Edina, MN); isomer shifts are referenced to iron metal at room temperature.

Results and Discussion

Synthetic routes leading to new MFe_3S_4 single cubane clusters **1**−**5** and **8**−**11** are outlined in Figures 1 and 2 and X-ray structures are depicted in Figures 3 and 4. Because of the large number of bond angles and distances in the structures of such clusters, metric data are restricted to the mean values of bond distances in Table 2. Mössbauer parameters and redox potentials are contained in Table 3. Prior and subsequent descriptions of clusters as "trigonal" refer to idealized geometric symmetry and not to crystallographically imposed symmetry (not observed here) nor necessarily to core electron distribution.

VFe_3S_4 Clusters. The synthetic procedure is based on displacement of solvate ligands in cluster **6**, which is readily formed by self-assembly from simple reactants.[22,23] Reaction 1 proceeds readily to afford **8** (38%).

$$[(DMF)_3VFe_3S_4Cl_3]^- + Li(Tpms) \rightarrow [(Tpms)VFe_3S_4Cl_3]^{2-} + Li^+ + 3DMF \quad (1)$$

This cluster undergoes precedented ligand substitution reactions at the iron sites to afford thiolate (**9**, **10**) and aryloxide (**11**) clusters (≳50%, Figure 1). Recently prepared tris(pyrazolyl)methanesulfonate,[28] a simple derivative of the well-studied tris(pyrazolyl)methanes[30] and, as the hydrotris(pyrazolyl)borates a facial monoanionic ligand,[30] was employed in reaction 1 with the hope of obtaining a water-soluble salt of **8**. However, $(Me_4N)_2$[**8**], while freely soluble in the usual polar organic solvents, is not appreciably soluble in water. Proof of clusters **8** and **9** is provided by X-ray structures (Figure 3). The structures of **7**−**9**, which contain the $[VFe_3S_4]^{2+}$ core, are essentially indistinguishable from one another (Table 2) and, in terms of core dimensions, from **6** [22] and the recently reported $[(MeCN)_3VFe_3S_4Cl_3]^-$,[31] the only other trigonal clusters available for comparison.

(30) Reger, D. L. *Comments Inorg. Chem.* **1999**, *21*, 1−28.

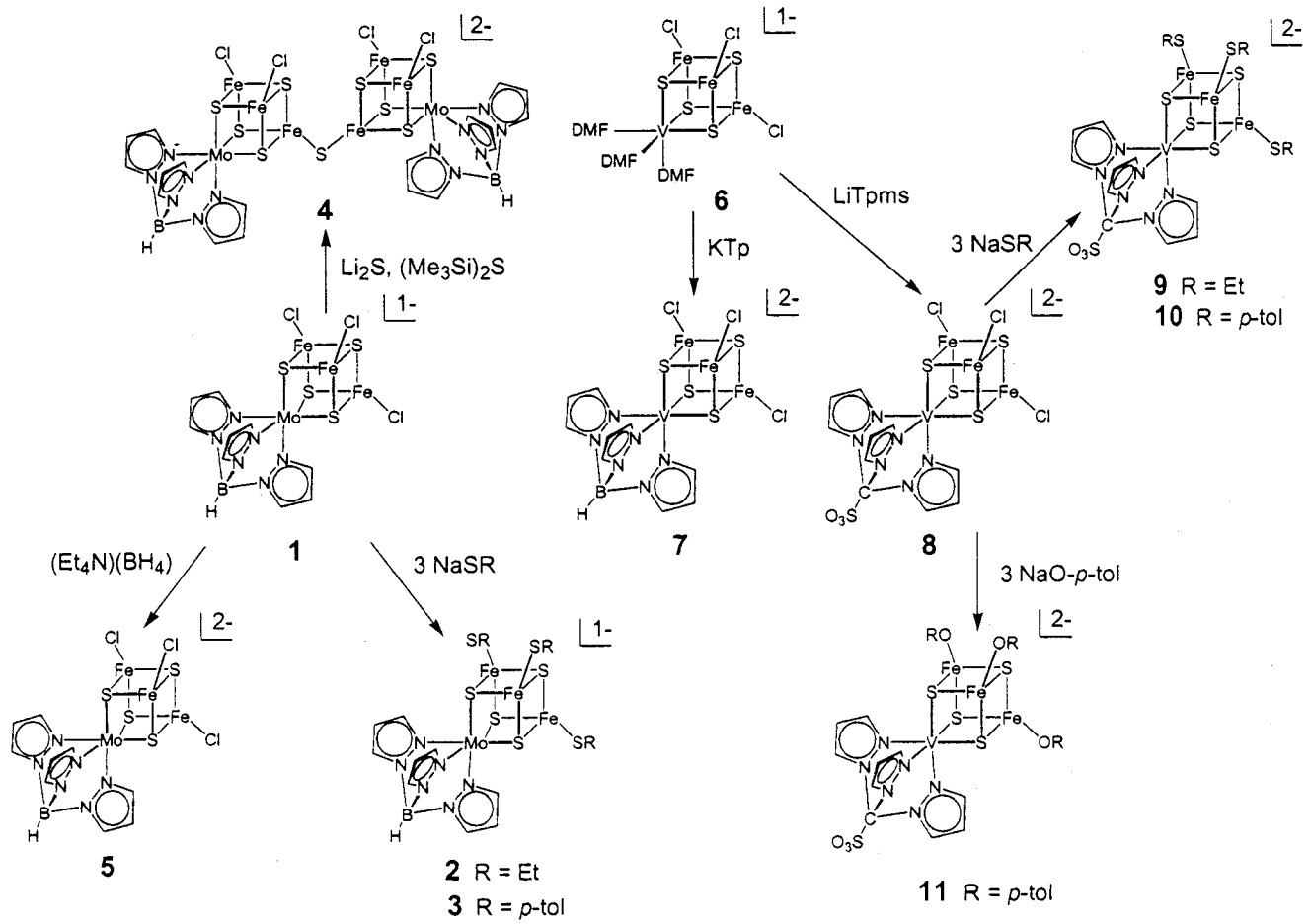

Figure 1. Synthetic scheme in acetonitrile for the preparation of trigonally symmetric MFe_3S_4 clusters with M = Mo (**2**−**5**) and V (**7**−**11**) based on **1** and **6**, respectively. The preparations of **6** and **7** have been previously reported; for the preparation of **1**, cf. Figure 2.

Table 2. Mean Values of Selected Bond Distances (Å) for Single Cubanes

	M−N	M−S	Fe−S	M-Fe	Fe−Fe	Fe−Cl/SEt
$[(Tp)MoFe_3S_4Cl_3]^-$ (**1**)	2.209(4)	2.343(2)	2.264(2)	2.731(1)	2.719(2)	2.189(2)
$[(Tp)MoFe_3S_4(SEt)_3]^-$ (**2**)	2.224(6)	2.355(3)	2.263(3)	2.733(1)	2.688(1)	2.232(3)
$[(Tp)MoFe_3S_4Cl_3]^{2-}$ (**5**)	2.236(5)	2.368(1)	2.282(2)	2.735(1)	2.719(1)	2.254(2)
$[(Meida)MoFe_3S_4Cl_3]^{2-}$ (**12**)[a]	N/A	2.348(4)	2.268(4)	2.730(2)	2.733(2)	2.226(4)
$[(Tp)VFe_3S_4Cl_3]^{2-}$ (**7**)[b]	2.196	2.302	2.251	2.755	2.670	2.232
$[(Tpms)VFe_3S_4Cl_3]^{2-}$ (**8**)	2.167(4)	2.331(1)	2.274(1)	2.755(1)	2.708(1)	2.231(2)
$[(Tpms)VFe_3S_4(SEt)_3]^{2-}$ (**9**)	2.177(4)	2.334(1)	2.277(1)	2.753(1)	2.726(1)	2.281(1)

[a] Reference 19. [b] Reference 24. These data were reported in Supporting Information; esd values were not given.

$MoFe_3S_4$ Clusters. The only known route to single cubanes prior to this work is outlined in Figure 2.[17,18] The procedure involves disruption of the iron/thiolatebridge of the indicated double cubane with a suitable catechol in reaction 2 of uncertain stoichiometry, cleavage of the thiolate-bridged double cubane product to a single cubane by reaction 3 in a coordinating solvent, substitution of terminal thiolate ligands with chloride in reaction 4 to prevent their removal in the next step, and displacement of bound catechol with the desired protonated ligand in reaction 5.[15,19]

$$[(Cl_4cat)(solv)MoFe_3S_4Cl_3]^{2-} + H_2(Meida) \rightarrow [(Cl_4cat)(solv)MoFe_3S_4Cl_3]^{2-} + Cl_4catH_2 \quad (5)$$

$$2[(Tp)MoS(S_4)]^- + 6FeCl_2 + 6NaSEt + 2PPh_3 \rightarrow 2[(Tp)MoFe_3S_4Cl_3]^- + 3EtSSEt + 2Ph_3PS + 6NaCl \quad (6)$$

With product cluster **12** as an example, the overall yield from the initial double cubane is ca. 45% in four steps. The entire procedure, including cluster purification at each step, requires no less than 1 week. Here we offer an improvement in the form of reaction 6 (Figure 2) with the apparent stoichiometry indicated. This reaction is based on the Mo(IV) sulfido complex **13** recently reported by Seino et al.[27] This complex is prepared in 75% yield from $[(Tp)Mo(CO)_3]^-$ and elemental sulfur and is analogous to $[(Tp^*)MoCl(S_4)]$ described by Young et al.[32] over 10 years before. We initially utilized the latter complex but obtained the desired cluster in low yield (<10%). We anticipate that reaction 6, which affords **1** in 75% yield, is capable of extension to other single cubanes

(31) Zhu, H.-P.; Liu, Q.-T.; Chen, C.-N. *Chin. J. Struct. Chem.* **2001**, *20*, 19−23.
(32) Young, C. G.; McInerney, I. P.; Bruck, M. A.; Enemark, J. H. *Inorg. Chem.* **1990**, *29*, 412−416.

Table 3. Mössbauer Parameters and Redox Potentials of MFe_3S_4 Clusters (M = V, Mo)

	mm/s		V vs SCE	
cluster	δ[a,b]	ΔE_Q[c]	$E_{1/2}$(ox)[d]	$E_{1/2}$(red)
$[(Tp)VFe_3S_4Cl_3]^-$ [e]	0.43	1.19		−0.11
$[(Tp)VFe_3S_4Cl_3]^{2-}$ [e] (**7**)	0.65(1), 0.50(2)	1.15(1), 1.10(2)	−0.11	−1.40 [g]
$[(Tpms)VFe_3S_4Cl_3]^{2-}$ (**8**)	0.53	1.20	0.06	−1.22 [g]
$[(Tpms)VFe_3S_4(SEt)_3]^{2-}$ (**9**)	0.46	1.10	−0.47	−1.58
$[(Tpms)VFe_3S_4(S\text{-}p\text{-}tol)_3]^{2-}$ (**10**)	0.46	1.24	−0.30	−1.38
$[(Tpms)VFe_3S_4(O\text{-}p\text{-}tol)_3]^{2-}$ (**11**)	f		−0.25	−1.40
$[(Tp)MoFe_3S_4Cl_3]^-$ (**1**)	0.51(2), 0.46(1)	1.09(2), 0.61(1)		−0.57
$[(Tp)MoFe_3S_4(SEt)_3]^-$ (**2**)	0.39	1.02		−0.96
$[(Tp)MoFe_3S_4Cl_3]^{2-}$ (**5**)	0.62(1), 0.59(2)	1.15(1), 0,62(2)	−0.57	−1.68 [g]
$[(Meida)MoFe_3S_4Cl_3]^{2-}$ [h] (**12**)	f			−0.81
$\{[(Tp)MoFe_3S_4Cl_2]_2S\}^{2-}$ (**4**)	f		−0.79	−1.08
$\{[(Meida)MoFe_3S_4Cl_2]_2S\}^{4-}$ [h] (**14**)	f		−1.01	−1.34

[a] ±0.02 mm/s at 4.2 K, referenced to Fe metal at room temperature. [b] 77 K. [c] ±0.03 mm/s. [d] Acetonitrile solution, 298 K. [e] Reference14; δ values at 80 K. [f] Not measured. [g] Irreversible, E_{pc}. [h] Reference 15, Me_2SO solution.

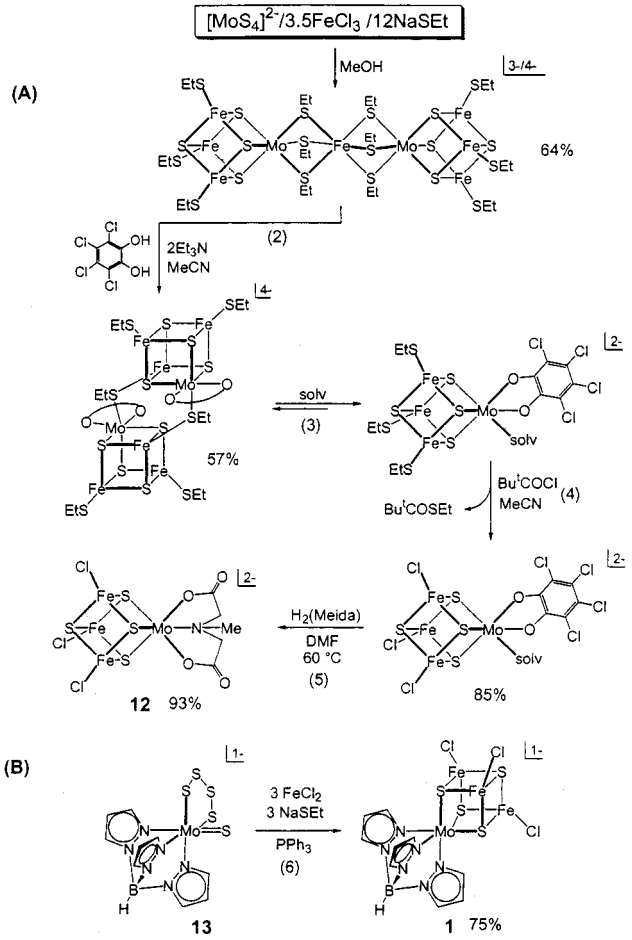

Figure 2. Synthesis of $[MoFe_3S_4]^{3+}$ single cubanes: (A) conventional method illustrated with product cluster $[(Meida)MoFe_3S_4Cl_3]^{2-}$ (**12**); (B) method introduced here using $[(Tp)MoS(S_4)]^-$ (**13**) as a precursor to $[(Tp)MoFe_3S_4Cl_3]^-$ (**1**).

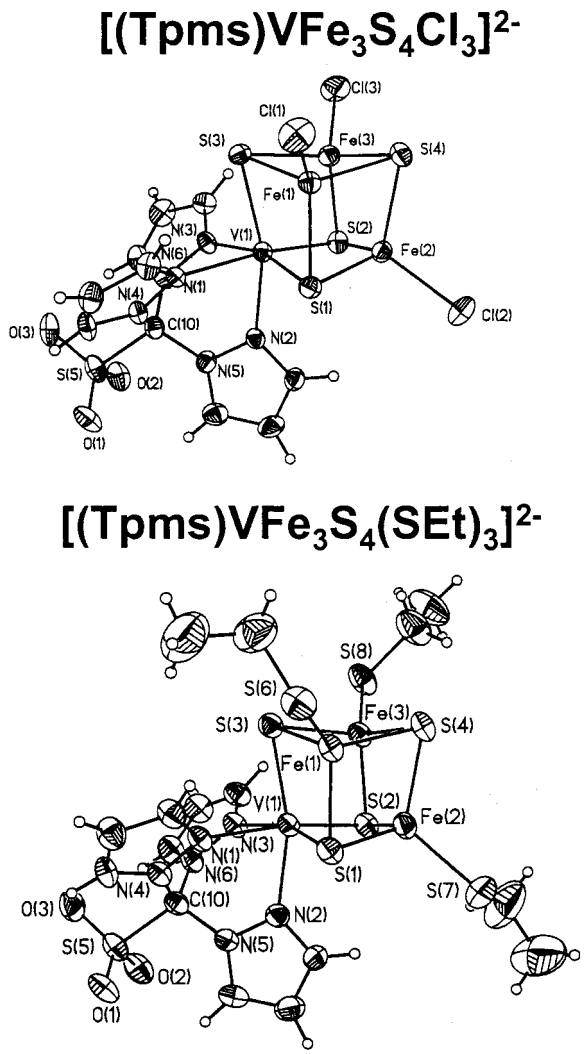

Figure 3. Structures of $[(Tpms)VFe_3S_4Cl_3]^{2-}$ (**8**) and $[(Tpms)VFe_3S_4(SEt)_3]^{2-}$ (**9**), showing 50% probability ellipsoids and atom labeling schemes.

with variant ligands at the molybdenum site. While this work was in progress, Han et al.[33] reported the preparation of $MoFe_3S_4$ cubanes by the reaction of $[(Cl_4cat)Mo(O)FeS_2Cl_2]^{2-}$ and $[Fe_2S_2Cl_4]^{2-}$.

With cluster **1** in hand, thiolate complexes **2** and **3** are readily obtained by ligand substitution. As is the case with all new clusters in this work, ^1H NMR spectra are consistent with trigonal symmetry. With **2**, for example, a single set of Tp resonances is observed together with one thiolate methylene (65.5 ppm) and methyl (5.67 ppm) signal. Clusters of the type $[(cat)(solv)MoFe_3S_4(SEt)_3]^{2-}$, which have fluxional 3-fold symmetry owing to rapid solvate dissociation and

(33) Han, J.; Koutmos, M.; Al-Ahmad, S.; Coucouvanis, D. *Inorg. Chem.* **2001**, *40*, 5985−5999.

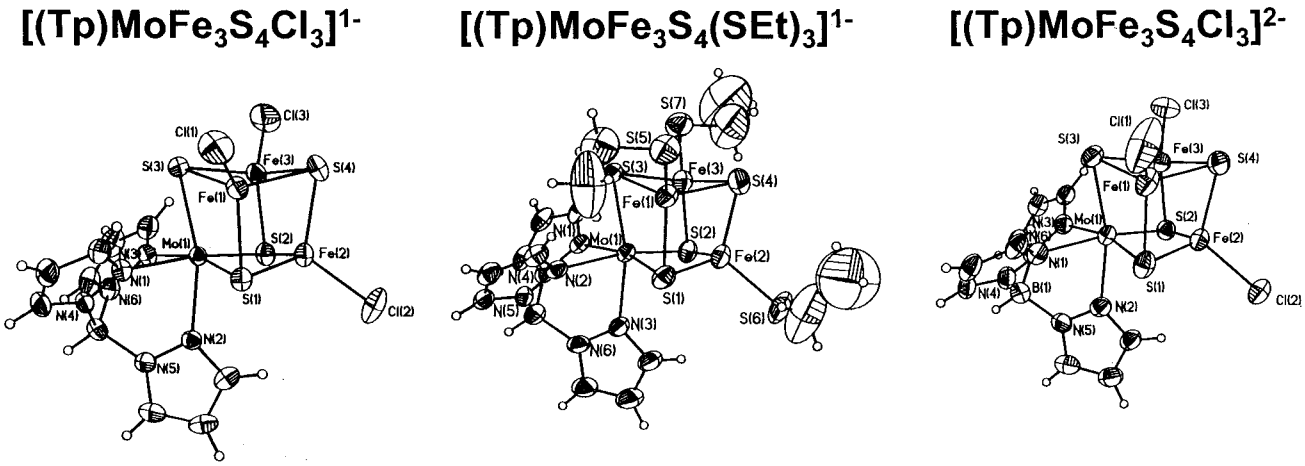

Figure 4. Structures of $[(Tp)MoFe_3S_4Cl_3]^-$ (**1**), $[(Tp)MoFe_3S_4(SEt)_3]^-$ (**2**), and $[(Tp)MoFe_3S_4Cl_3]^{2-}$ (**5**), showing 50% probability ellipsoids and atom labeling schemes.

rebinding, also exhibit one set of strongly downfield-shifted ethyl resonances.[17,18]

Redox Series. The majority of isolated $[VFe_3S_4]^{2+}$ ($S = 3/2$) clusters, obtained by self-assembly synthesis, show a chemically reversible oxidation ($i_{pa}/i_{pc} \approx 1$) to the $[VFe_3S_4]^{3+}$ ($S = 0$) and an irreversible reduction to the $[VFe_3S_4]^+$ state.[22,23] However, $[(Tp)VFe_3S_4(LS_3)]^{2-}$ [23] and **9**−**11** each exhibit a reversible oxidation and reduction (Table 3), thereby defining the series 7

$$[VFe_3S_4]^{3+} \rightleftharpoons [VFe_3S_4]^{2+} \rightleftharpoons [VFe_3S_4]^{+} \qquad (7)$$

$$[MoFe_3S_4]^{4+} \rightleftharpoons [MoFe_3S_4]^{3+} \rightleftharpoons [MoFe_3S_4]^{2+} \qquad (8)$$

for the same molecule. The potential of −0.11 V for the oxidation of **7** facilitates ready chemical oxidation to $[(Tp)VFe_3S_4Cl_3]^-$.[14] The $[VFe_3S_4]^{3+}$ state has now been established in the latter cluster, $[VFe_3S_4(S_2CNEt_2)_4]^-$,[34] and the double cubane $[V_2Fe_6S_8(SEt)_9]^{3-}$.[35] The first comparative effect of Tp and Tpms ligands on redox potentials is indicated by the observation that **7** is easier to oxidize than **8** by 170 mV at parity of iron terminal ligands. Comparison of **7** or **8** with $[(Tp)VFe_3S_4Cl_3]^-$ reveals no cluster trends in metric parameters above the 3σ level.[14] Evidently, any structural differences are obscured by electron delocalization. However, as will be seen, electron density at the iron sites is appreciably different in the $[VFe_3S_4]^{2+,3+}$ oxidation levels by Mössbauer spectroscopy.

Clusters in the $[MoFe_3S_4]^{3+}$ ($S = 3/2$) oxidation state are readily formed by self-assembly. Collective synthetic and electrochemical results support redox series 8, especially for the phosphine clusters $[(Cl_4cat)(MeCN)MoFe_3S_4(PR_3)_3]^{1+,0,1-}$, which are linked by reversible reactions.[9] Only the $[MoFe_3S_4]^{2+}$ state in that series has been isolated. None of the clusters examined here show two reversible redox steps (Table 3). However, the reduction of **1** at the mild potential of −0.57 V suggested isolation of a cluster with the same ligation mode as its one-electron oxidized form and thus ideally suitable for the structure comparison. Treatment of **1** with borohydride led to the isolation of $(Bu_4N)_2$[**5**] (67%). Earlier, $[(cat)(EtCN)MoFe_3S_4(S\text{-}p\text{-}C_6H_4Cl)_3]^{3-}$ with the $[MoFe_3S_4]^{2+}$ ($S = 2$) core was isolated,[36] but its structure was not determined. The trigonally symmetric structures of **1**, **2**, and **5** are set out in Figure 3. Comparison of mean bond lengths of **1** and **5** (Table 2) reveal a trend of slightly increased Mo−N, Mo−S, and Fe−S bond lengths (ca. 0.02−0.03 Å), suggesting that the added electron has antibonding character. Further, the increase of 0.065 Å in Fe−Cl distances is indicative of increased Fe(II) core character inasmuch as the Shannon radius of tetrahedral Fe(II) is 0.14 Å larger than for tetrahedral Fe(III).[37] Similar trends are usually observed in comparing the structures of $[Fe_4S_4]^{2+,1+}$ clusters with terminal thiolate ligands.[38−40]

Electron Delocalization and Oxidation States. We have most recently addressed these issues with VFe_3S_4 clusters,[14] using Mössbauer spectroscopy and an empirical linear correlation $\delta = 1.36-0.36s$ between isomer shift δ at 4.2 K and (mean) oxidation state s for tetrahedral $FeS_{4-n}(SR)_n$ sites.[35] The Mössbauer spectrum of **1**, consisting of two overlapping quadrupole doublets (Figure 5) is shown as an example. Determination of s leads to the oxidation state of the heterometal by difference if the core charge is known. We assume the same difference obtains between iron oxidation states if one sulfur ligand is replaced by chloride. The difference in mean values $\delta(\mathbf{5}) - \delta(\mathbf{1}) = 0.60 - 0.49 = 0.11$ mm/s (Table 3) is close to the value $0.36/3 = 0.12$ mm/s predicted for the isomer shift per iron atom upon one-electron reduction. Using as a reference the delocalized cluster $[Fe_4S_4Cl_4]^{2-}$ ($Fe^{2.5+}$, $\delta = 0.51$ mm/s), we estimate $0.51 - 0.36/2 = 0.33$ mm/s for the hypothetical $Fe^{3+}{}_3$

(34) Deng, Y.; Liu, Q.; Chen, C.; Wang, Y.; Cai, Y.; Wu, D.; Kang, B.; Liao, D.; Cui, J. *Polyhedron* **1997**, *16*, 4121−4128.
(35) Cen, W.; Lee, S. C.; Li, J.; MacDonnell, F. M.; Holm, R. H. *J. Am. Chem. Soc.* **1993**, *115*, 9515−9523.
(36) Mizobe, Y.; Mascharak, P. K.; Palermo, R. E.; Holm, R. H. *Inorg. Chim. Acta* **1983**, *80*, L65-L67.
(37) Shannon, R. D. *Acta Crystallogr.* **1976**, *A32*, 751−767.
(38) Hagen, K. S.; Watson, A. D.; Holm, R. H. *Inorg. Chem.* **1984**, *23*, 2984−2990.
(39) Carney, M. J.; Papaefthymiou, G. C.; Whitener, M. A.; Spartalian, K.; Frankel, R. B.; Holm, R. H. *Inorg. Chem.* **1988**, *27*, 346−352.
(40) Carney, M. J.; Papaefthymiou, G. C.; Frankel, R. B.; Holm, R. H. *Inorg. Chem.* **1989**, *28*, 1497−1503.

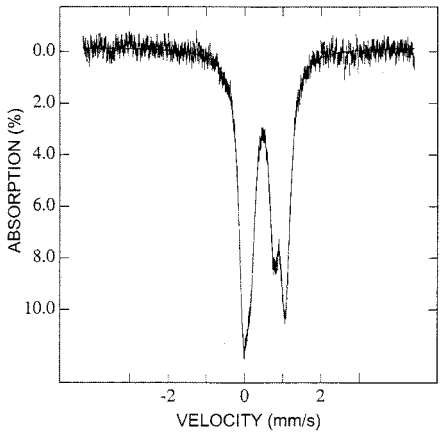

Figure 5. Zero-field Mössbauer spectrum of $[(Tp)MoFe_3S_4Cl_3]^-$ (**5**). The solid line is a fit to the data using the parameters listed in Table 3.

subcluster, 0.33 + 0.12 = 0.45 mm/s for the $Fe^{3+}{}_2Fe^{2+}$ subcluster, and 0.33 + (2)(0.12) = 0.57 for the $Fe^{3+}Fe^{2+}{}_2$ subcluster. We suggest that **1** is reasonably described as $[Mo^{3+}Fe^{3+}{}_2Fe^{2+}S_4]^{3+}$ and **5** as $[Mo^{3+}Fe^{3+}Fe^{2+}{}_2S_4]^{2+}$, in which case the redox event is largely confined to the delocalized Fe_3 subcluster and associated sulfur atoms. Some Mo participation in the MO occupied by the added electron is implied by the difference in Mo−N distances of 0.015 Å (Table 2), which is, however, marginal at the 3σ level. Recently, using the same procedure, we have concluded that $[(Tp)VFe_3S_4Cl_3]^-$ and **7** may be formulated as $[V^{3+}Fe^{3+}{}_2Fe^{2+}S_4]^{3+}$ and $[V^{3+}Fe^{3+}Fe^{2+}{}_2S_4]^{2+}$, respectively; i.e., redox changes are again mainly associated with the Fe_3 subcluster.[14] The procedure utilizes Fe^{3+} as surrogate for the heterometal ion in the treatment of isomer shifts. Because of the small differences in isomer shifts and use of the empirical isomer shift equation, we offer the foregoing as the best current approximations of charge distribution in these delocalized clusters. Comparisons are best made within a given heterometal series. The small difference in isomer shift of 0.04−0.06 mm/s between **1** and **7/8** implies, but cannot be said to prove, that the isoelectronic cores $[MoFe_3S_4]^{3+}$ and $[VFe_3S_4]^{2+}$ contain Fe_3 fragments in the same oxidation state.

Sulfide-Bridged Double Cubane. Our previous studies of the formation of sulfide-bridged double cubanes have been complicated by the mirror symmetry of the single cubane precursors $[(Meida)MoFe_3S_4L_3]^{2-}$.[15,16] Bridging of these cubanes by a sulfide affords a combination of four possible geometrical isomers by statistical combination at one of two types of iron sites, designated m′ and m″. Trigonally symmetric cubanes may be combined in only one way, resulting in a single isomer containing two equivalent clusters with iron sites in a ratio of 2(m″):1(m′). When cluster **1** is treated with varying equivalents of $(Me_3Si)_2S$ in acetonitrile, and the reaction followed by ^1H NMR (Figure 6), the indicated signals of double cubane **4** in a 2:1 ratio develop. When reaction 9 is carried out on preparative scale with less

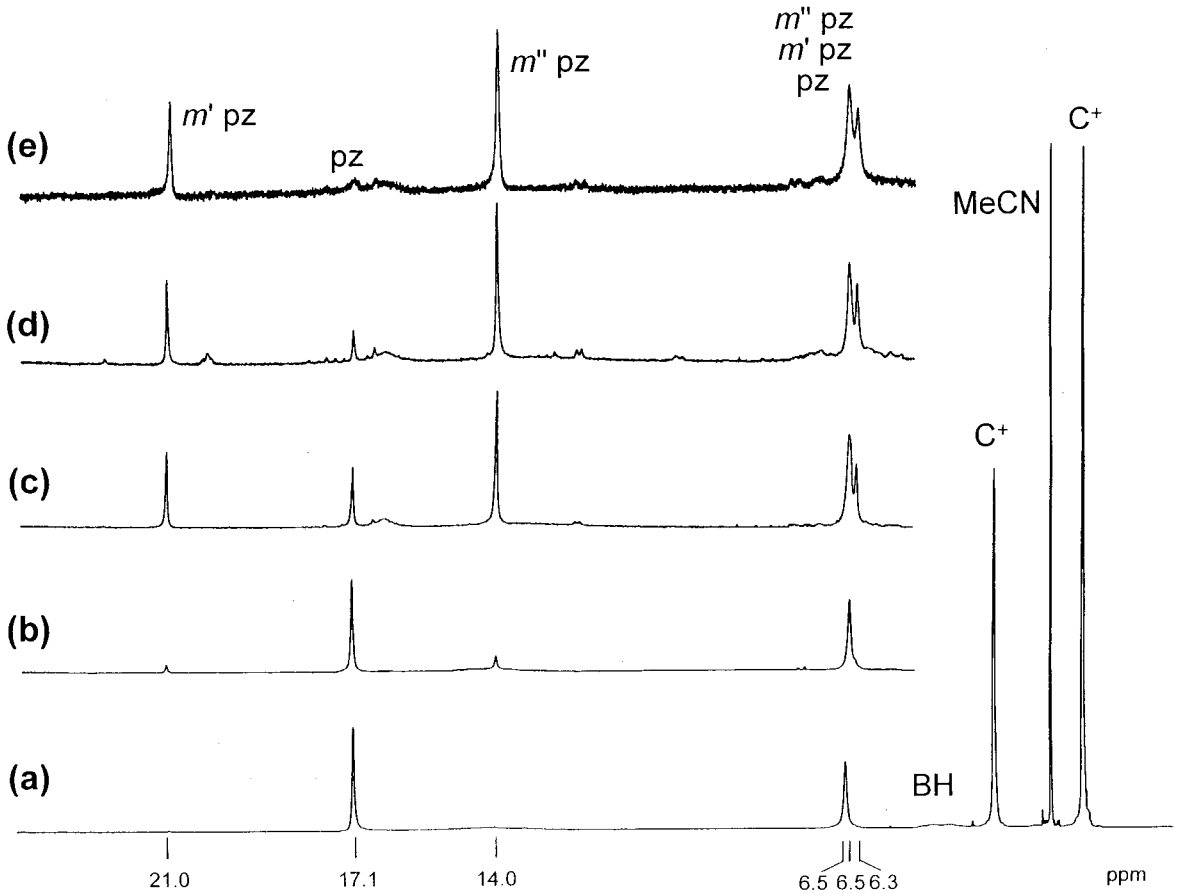

Figure 6. ^1H NMR spectra in CD_3CN: (a) $[(Tp)MoFe_3S_4Cl_3]^-$ (**1**); (b−d) **1** + 0.26, 0.50, and 0.66 equiv of $(Me_3Si)_2S$; (e) $\{[(Tp)MoFe_3S_4Cl_2]_2S\}^{2-}$ (**4**) prepared by the reaction of **1** and Li_2S in acetonitrile. (pz = pyrazolyl C−H; $C^+ = Et_4N^+$.)

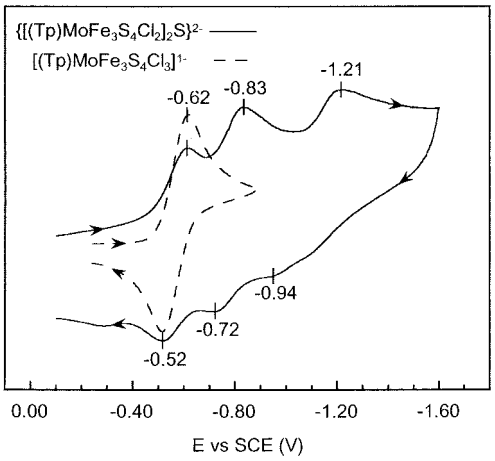

Figure 7. Cyclic voltammograms (100 mV/s) in acetonitrile solutions of a mixture of $[(Tp)MoFe_3S_4Cl_3]^-$ (**1**) and $\{[(Tp)MoFe_3S_4Cl_2]_2S\}^{2-}$ (**4**) (solid line) and of **1** measured separately (dashed line). Peak potentials vs SCE are indicated.

than 1/2 equiv of Li_2S, a mixture containing only **4** and initial cluster **1** is generated.

$$2[(Tp)MoFe_3S_4Cl_3]^- + Li_2S \rightarrow \{[(Tp)MoFe_3S_4Cl_2]_2S\}^{2-} + 2LiCl \quad (9)$$

When the amount of Li_2S approaches or exceeds 1/2 equiv, an unidentified impurity together with **4** is observed. With a large excess of reagent (ca. 1:1), $(Et_4N)_2$[**4**] (91%) was isolated in analytical purity. The ^{1}H NMR spectrum of the cluster product is identical to that formed with $(Me_3Si)_2S$. We have been unable to obtain diffraction-quality crystals of this compound. However, cyclic voltammetry provides satisfactory evidence for the double cubane formulation. In one experiment, a mixture of **1** and **4** in acetonitrile was generated. The process at $E_{1/2} = -0.57$ V is due to **1** and the remaining two features, at $E_{1/2} = -0.79$ and -1.08 V, arise from **4** (Figure 7). The corresponding potentials for single cubane **12** and double cubane **14**, -0.81 and $-1.08/-1.34$ V,[15] are more negative because of the higher negative charge. The separation of the two reduction steps of double cubanes, 330 (**14**) and 290 mV (**4**) are quite close, as would be expected for structures in which the redox sites are identically bridged at nearly the same distances. Earlier, we had connected **14** and other double cubanes showing the two reduction steps to parent ions of the correct mass in their electrospray mass spectra.[15] Further, all double cubanes of type $\{[(Meida)MoFe_3S_4L_2]_2S\}^{4-}$, as well as $\{[Fe_4S_4Cl_3]_2S\}^{4-}$ of proven structure[41] and other Fe_4S_4 double cubanes, exhibit two successive reduction steps separated by 230−330 mV.[15,16] As yet, we have not been able to obtain pure double cubanes by coupling the vanadium clusters **7** and **8**.

Summary

The following are the principal results and conclusions of this investigation, together with certain results from previous studies.

(1) A series of trigonally symmetric MFe_3S_4 single cubanes has been prepared with the facial tridentate ligands tris(pyrazolyl)methanesulfonate (M = V) or hydrotris(pyrazolyl)borate (M = Mo) at the heterometal site. Vanadium clusters are obtained by solvate ligand displacement of $[(DMF)_3VFe_3S_4Cl_3]^-$. The molybdenum cluster $[(Tp)MoFe_3S_4Cl_3]^-$ (75%) was prepared by the reaction of $[(Tp)MoS(S_4)]^-$ [27] and $FeCl_2$/NaSEt in a new method that obviates the previous multistep procedure that leads to clusters with mirror symmetry. This method may be capable of extension to clusters with other ligands and metals. Additional clusters are afforded by chloride ligand substitution reactions, and $[(Tp)MoFe_3S_4Cl_3]^{2-}$ was isolated from borohydride reduction of $[(Tp)MoFe_3S_4Cl_3]^-$.

(2) Structures of five clusters in (1) were established by X-ray determinations, including the pair $[(Tp)MoFe_3S_4Cl_3]^{1-,2-}$ which provided the first structure comparison of $[MoFe_3S_4]^{3+,2+}$ clusters at exact parity of ligation. Most core bond lengths and terminal Fe−Cl distances increase upon reduction, indicating that the added electron is antibonding and delocalized over the Fe_3 subcluster and associated sulfur atoms.

(3) Collective electrochemical and synthetic results from this and other studies establish the accessible core oxidation state ranges $[VFe_3S_4]^{3+,2+,1+}$ and $[MoFe_3S_4]^{4+,3+,2+}$, with stabilities strongly dependent on ligand type. Examples of all clusters except $[MoFe_3S_4]^{4+}$ have been isolated.

(4) Analysis of ^{57}Fe isomer shifts leads to the approximate charge distributions descriptions $[Mo^{3+}Fe^{3+}{}_2Fe^{2+}S_4]^{3+}$ for $[(Tp)MoFe_3S_4Cl_3]^-$ and $[Mo^{3+}Fe^{3+}Fe^{2+}{}_2S_4]^{2+}$ for $[(Tp)MoFe_3S_4Cl_3]^{2-}$, indicating that the added electron is largely delocalized over the Fe_3 fragment.

(5) Reaction of $[(Tp)MoFe_3S_4Cl_3]^-$ with $(Me_3Si)_2S$ or with excess Li_2S affords the double cubane $\{[(Tp)MoFe_3S_4Cl_2]_2(\mu_{2-}S)\}^{2-}$ whose sulfide-bridged structure was established by ^{1}H NMR and a 290 mV separation of sequential reduction steps, a value closely comparable with previously reported double cubanes of higher negative charge.

Access to trigonally symmetric single cubanes and double cubanes from which they are derived eliminates isomeric mixtures encountered in earlier work and may be of substantial assistance in the preparation, purification, and crystallization of new structural types of M−Fe−S clusters.

Acknowledgment. This research was supported by NIH Grant GM 28856. We thank Drs. C. Achim and H. Zhou for useful discussions and experimental assistance. C.C.M. is an NIH Postdoctoral Fellow.

Supporting Information Available: Text describing preparations and figures showing structures of compounds not described in detail, and X-ray crystallographic files in CIF format for the structure determinations of the five compounds in Table 1 and those specified as Other Compounds in the Experimental Section. This material is available free of charge via the Internet at http://pubs.acs.org.

IC011106D

(41) Challen, P. R.; Koo, S. M.; Dunham, W. R.; Coucouvanis, D. *J. Am. Chem. Soc.* **1990**, *112*, 2455−2456.